Correlation between the ionic potential and thermal stability of metal borohydrides: First-principles investigations

Piotr Błoński* and Zbigniew Łodziana†

Institute of Nuclear Physics, Polish Academy of Sciences, ul. Radzikowskiego 152, PL-31-342 Kraków, Poland

(Received 30 June 2014; revised manuscript received 6 August 2014; published 25 August 2014)

Metal borohydrides are intensively studied because of their potential applications as versatile hydrogen storage. The relation between the formation enthalpy and the Pauling electronegativity established for these materials [Phys. Rev. B **74**, 045126 (2006)] led to the idea of developing mixed-cation compounds that may provide a route for tuning the thermodynamic stability of metal borohydrides. We report a systematic *ab initio* investigation of the single-metallic and bimetallic borohydrides, and via an examination of the Born effective charges we provide insight into the physical mechanism determining their stabilities. We show that the decreasing stability of metal borohydrides follows the increasing polarizing ability of the cationic bonding component, expressed as the square root of the cation's dynamical charge divided by its radius in coordinated anion polyhedra around the cation. The charge-to-size ratio thus provides a simple yet physically sound measure of the stabilities of metal borohydrides that can be obtained in relatively simple calculations.

DOI: 10.1103/PhysRevB.90.054114 PACS number(s): 61.50.Ah, 61.50.Lt, 63.20.−e, 71.15.Mb

I. INTRODUCTION

Metal borohydrides $M(BH_4)_n$, where n denotes the valence of the metal M, are considered as promising solid-state hydrogen storage candidates due to their high hydrogen content [1]. Unfortunately, many of these compounds exhibit both unfavorable thermodynamic properties and slow kinetics for direct technological application (see, e.g., Ref. [2] and references therein).

Despite intensive theoretical and experimental research efforts towards a better comprehension of the chemistry of metal borohydrides, the mechanisms governing their stabilities are not well understood [2]. In $M(BH_4)_n$, the $[BH_4]^-$ anions are charged balanced by the metal cations with the valence n, M^{n+} [3–6]. A number of publications [2,7,8] report that the stability of metal borohydrides decreases as the Pauling electronegativity χ_P of a metal increases. Thus, a partial substitution of the metal cation by the element with larger electronegativity would compromise the charge transfer from M^{n+} to $[BH_4]^-$, hence weakening the internal covalent bonding of the anion and decreasing the decomposition temperature T_{dec} [8]. This drives a recent interest towards the synthesis of mixed-cation borohydrides $MM'(BH_4)_n$ (see, e.g., Refs. [2,8,10–13]). Very recently, the combined first-principles and experimental study by Łodziana *et al.* [9] has revealed a relation between Pauling electronegativity of metal cation and boron chemical shift in metal borohydrides, which can serve as a simple method for determining the stability of poorly crystalline materials.

Electronegativity is a measure of the ability of an atom to attract a bonding pair of electrons. Note that electronegativity is not directly measurable, although it is closely related to many chemical properties as bond energies, electron affinities, ionization energies, etc. Owing to the correlations between electronegativity and the aforementioned properties, a number of electronegativity scales have been proposed over the past ~80 years (see Ref. [14]). The original Pauling scale [15,16] is the most commonly used.

Pauling's electronegativity scale is based on the empirical fact that the energy of a bond $D(A\text{-}B)$ between atoms A and B is generally larger than the additive mean of the energies of the bonds $D(A\text{-}A)$ and $D(B\text{-}B)$. The difference Δ_{A-B} between the bond energy $D(A\text{-}B)$ and the arithmetic (or geometrical) mean of energies $D(A-A)$ and $D(B-B)$ increases with the increasing difference in the electronegativity values of atoms A and B. The relationship proposed by Pauling is $\Delta_{A-B} = 30(\chi_A - \chi_B)^2$, and the bond energy (in kcal/mol) is given by $D(A\text{-}B) = [D(A\text{-}A) + D(B\text{-}B)]/2 + \Delta_{A-B}$ [16]. For compounds of the MX_n type, for which a single bond energy $M\text{-}M$ is unknown, Δ can be approximately calculated from the enthalpy of formation of MX_n [17].

Four years before Pauling's concept of electronegativity scale, Cartledge introduced the quantity which he called the ionic potential ϕ [18]. He was inspired by the concept of the Polish chemist Fajans of the formation of polar-covalent $\rightarrow$ covalent bonds via the progressive polarization of an idealized ionic bond [19,20]. Cartledge defined the ionic potential as the ratio of a cation's net charge to its radius. Large charges and small sizes of the cations increase the bond polarization. The charge-to-size ratio thus represents a "polarizing power" of the cations: it measures the magnitude of the anion electron cloud distortion. Subsequently, Cartledge demonstrated [18] that the square root of ionic potential $\phi^{0.5}$ is an important property of ions (e.g., it is directly related to the ionization potential) and closely related to many characteristics of crystals. In a consecutive paper, Cartledge showed [21] that the stabilities of a number of compounds sharing a common anion (oxides, halogens, sulfides, and nitrides) scale as an inverse of the ionic potential of cations. More recently, a similar relationship between thermal stability and the ionic potential in zeolites has been revealed [22]. A strong positive correlation can be found for a plot of the numerical values for $\phi^{0.5}$ for the main-block elements versus the corresponding Pauling electronegativities [18]. Since the difference in atoms' electronegativity can be regarded as a measure of the degree of electron transfer between atoms on the chemical bond

*Corresponding author: Piotr.Blonski@ifj.edu.pl
†Zbigniew.Lodziana@ifj.edu.pl

formation, the ionic potential can serve as a electronegativity measure. This indicates that the square root of the ionic charge over its radius in crystal's coordinated polyhedra [23,24] must be firmly linked with its stability.

The quantification of the static charges associated with atoms/ions is usually based on the partitioning of the ground-state electron density into contribution from different atoms [25]. Within an extreme ionic limit, the static charges should be equal to the ionic nominal ones. In a mixed ionic-covalent compound, the charge transfer between ions is not complete, consequently, smaller than the nominal charges are expected. The dynamical charges (also called the Born effective charges) [26] are microscopically well defined as they measure the change of polarization induced by an ion displacement in zero macroscopic electric field. The dynamical charge of a given ion is a tensor reflecting its site symmetry. Within an extreme ionic limit, and for a rigid-ion model, the dynamical charge corresponds to the nominal static charge of the ion. When the ionic material is partially covalent, the displacement of a given ion induces a nonrigid displacement of the associated electronic charge. The borderline ionic-covalent character may lead to anomalous values of the Born effective charges [27]. Anomalously large ionic charges in ABO_3 oxides (e.g., $BaTiO_3$) that originate from the hybridization of $2p$ oxygen orbitals with the $4d$ or $5d$ orbitals of the B cation are striking examples [27]. Note that the Born effective charge tensor (BECT) depends on the long-range Coulomb interaction. As the longitudinal optical (LO) transverse optical (TO) splitting of the phonon dispersion curves also depends on the long-range Coulomb interaction, the Born effective charge is experimentally accessible. The BECT can be calculated within density functional perturbation theory (DFPT). Alternatively, the modern theory of the macroscopic polarization allows one to calculate Born charges as Berry phase [28]. To the best of our knowledge, the available literature reporting the ionic charges in metal borohydrides is comparatively scarce. Miwa *et al.* [3,6] have calculated the Born effective charge tensor components for selected alkali (Li, Na) [3,7] and alkaline-earth metal (Ca) [6] borohydrides to elucidate the bonding character in these compounds.

In this work, we use density functional theory (DFT) [29] to systematically investigate the relation between the experimental decomposition temperatures of $M(BH_4)_n$ and $MM'(BH_4)_n$, the Pauling electronegativity, and the ionic potential of cations for a technologically significant class of tetrahydroborates. The results obtained using static Bader and dynamical Born effective charges are confronted.

II. COMPUTATIONAL DETAILS

The first-principles DFT calculations reported here were performed using the Vienna *ab initio* simulation package (VASP) [30,31] with a plane-wave basis set (here containing components with energies up to 800 eV). The electron-ion interaction was treated by the projector-augmented-wave (PAW) method [31,32]. For the exchange correlation, the functional of Perdew, Burke, and Ernzerhof (PBE) is used [33] in the generalized-gradient approximation (GGA). The k-point sampling was performed on a dense Monkhorst-Pack [34] grid (see Table I).

For each compound, the representative crystalline phase was considered (Table I), and all structures were fully optimized with respect to both the lattice parameters and internal positions of atoms in the unit cell until the residual atomic forces are lower than 10 meV/Å. Simultaneously, the electronic degrees of freedom were relaxed until the change in the total energy between the successive iteration steps was smaller than 10^{-6} eV. Taking into account the variety of compounds studied here, the agreement between the calculated and experimental lattice parameters is very good. The deviation from the experimental data does not exceed a few percent. We have also checked that the structures are converged with respect to the k-point mesh and the cutoff energy E_{cut} for the plane-wave basis set.

TABLE I. Calculated lattice parameters (in Å and degrees) for representative metal borohydrides $M(BH_4)_n$ and mixed-cation $MM'(BH_4)_n$ compounds in the crystalline state. The initial structures are taken from references given in the last column. The second column lists the k-point meshes used for each compound.

Compound	k-point mesh	a_0	b_0	c_0	α,β,γ	Space group	Ref.
$LiBH_4$	$8\times10\times8$	7.34	4.36	6.54	90,90,90	$Pnma$	[35]
$NaBH_4$	$10\times10\times8$	4.34	4.34	5.88	90,90,90	$P4_2/nmc$	[36]
KBH_4	$10\times10\times8$	4.77	4.77	6.70	90,90,90	$P4_2/nmc$	[37]
$Be(BH_4)_2$	$4\times4\times6$	14.28	14.28	9.54	90,90,90	$I4_1cd$	[38]
$Mg(BH_4)_2$	$6\times4\times4$	9.95	11.21	11.91	90,90,90	$F222$	[39]
$Mg(BH_4)_2$	$6\times6\times4$	8.31	8.31	10.55	90,90,90	$I4_1/amd$	[39]
$Ca(BH_4)_2$	$6\times4\times6$	8.73	13.12	7.50	90,90,90	$Fddd$	[40]
$Al(BH_4)_3$	$2\times8\times8$	18.35	6.57	6.97	90,90,90	$Pna2_1$	[41]
$Sc(BH_4)_3$	$6\times6\times6$	10.29	10.29	10.29	90,90,90	$Pa\bar{3}$	[42]
$Y(BH_4)_3$	$6\times6\times6$	10.84	10.84	10.84	90,90,90	$Pa\bar{3}$	[43]
$Zr(BH_4)_4$	$8\times8\times8$	6.08	6.08	6.08	90,90,90	$P23$	[44]
$LiK(BH_4)_2$	$8\times10\times4$	7.87	4.46	13.78	90,90,90	$Pnma$	[10]
$NaY(BH_4)_2Cl_2$	$8\times6\times8$	6.73	8.37	6.71	90,89.8,90	$P2/c$	[11]
$NaSc(BH_4)_4$	$6\times4\times6$	8.16	11.97	9.11	90,90,90	$Cmcm$	[45]
$KSc(BH_4)_4$	$4\times6\times6$	12.70	8.42	9.14	90,90,90	$Pnma$	[46]
$KAl(BH_4)_4$	$6\times4\times4$	9.75	12.54	14.92	90,90,90	$Fdd2$	[12]

The Born dynamical-charge tensors [26] $\mathbf{Z}^*_{\kappa,\alpha\beta}$, measuring the linear polarization $\mathbf{P}_\beta$ induced in direction β in zero external field by a small displacement of atom κ in direction α, $\tau_{\kappa,\alpha}$, have been calculated within density functional perturbation theory. The isotropic component Z^*_κ of the BECT is equal to one-third of its trace. The convergence of the BECT calculations with respect to the k-point mesh and $E_{\rm cut}$ has been carefully analyzed (see Fig. S1 of the Supplemental Material [47]). Partitioning of the ground-state electronic density into contributions attributed to the different atoms (static charges) has been performed by means of Bader analysis [25,48,49].

The heat of formation ΔH of borohydride compounds has been calculated as the difference in total electronic energy ΔE of the products and the reactants. For example, $\Delta H(\mathrm{LiBH_4}) = \Delta E(\mathrm{LiBH_4}) - [\Delta E(\mathrm{Li}) + \Delta E(\mathrm{B}) + 2\Delta E(\mathrm{H_2})]$ refers to the calculated total ground-state energy of crystalline phases of solids and gas phase for H_2. Such a definition conforms with that used in previous reports on the electronegativity-stability relation, e.g., Ref. [7].

III. RESULTS AND DISCUSSION

A. Dynamic versus static ionic charges

The static Bader and dynamical Born effective charges on cations in single-cation borohydrides are compared in Fig. 1. For dual cation borohydrides only the values of effective charges are shown. All components of the BECT of the selected compounds studied in this work are reported in the Supplemental Material [47]. For alkali-metal compounds, the dynamical charges on cations are close to the nominal value of +1. The BH_4 complexes are ionized as anions fulfilling the acoustic sum rule within 0.03 e; this reflects the numerical accuracy of our calculations. In addition, we have also calculated Z^* for the high-temperature phases of $NaBH_4$ and KBH_4. The difference with respect to the charges in the low-temperature phases does not exceed 7%.

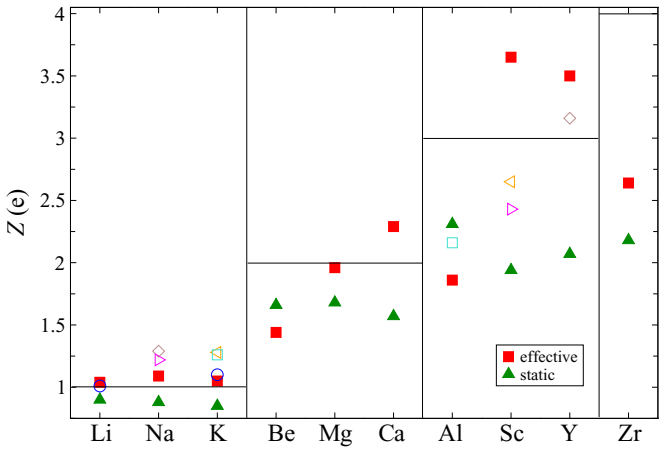

FIG. 1. (Color online) The static Bader and Born effective charges on metal cation calculated for $M(\mathrm{BH_4})_n$ ($n = 1$ to 4). For dual-cation borohydrides, only the Born charges are shown (open symbols). $\mathrm{LiK(BH_4)_2}$ (circles); $\mathrm{NaY(BH_4)_2Cl_2}$ (diamonds); NaSc(BH4)4 (triangles-right); KSc(BH4)4 (triangles-left); KAl(BH4)4 (squares). Vertical solid lines are used to separate metals of different valency (depicted by horizontal solid lines).

Among the remaining single-metal borohydrides investigated here, the Born effective charges can be divided into three groups: lower, equal, or larger than the nominal charges of cations. Only diagonal elements of $Z^*_{\rm Mg}$ in the $\mathrm{Mg(BH_4)_2}$ compound with $I4_1/amd$ symmetry are close to the nominal value of +2; in the $F222$ structure the dynamical charge on Mg is lower than the nominal one by 10%. In the α phase of $\mathrm{Ca(BH_4)_2}$ the dynamical charge on Ca is larger by 15% than the nominal charge of +2. $Z^*_{\rm Ca}$ in the β- and γ-$\mathrm{Ca(BH_4)_2}$ polymorphs are, respectively, larger by 17% and 18% than the nominal charge of +2. Also, in both trivalent d-block transition-metal borohydrides $\mathrm{Sc(BH_4)_3}$ and $\mathrm{Y(BH_4)_3}$, Z^*_M is larger than the nominal charge of +3 by 22% and 17%, respectively. For $\mathrm{Y(BH_4)_3}$, the effective charges in the high-temperature polymorph in $Fm\bar{3}$ symmetry agree with those of the low-temperature phase within 3%. For the bivalent $\mathrm{Be(BH_4)_2}$, trivalent $\mathrm{Al(BH_4)_3}$, and tetravalent $\mathrm{Zr(BH_4)_4}$, a strong reduction of the cation Born effective charges with respect to the nominal charge by 28% (Be), 38% (Al), and 34% (Zr), respectively, is found.

For the mixed-binary-cations systems, the Born effective charges on both cations change with respect to the charges of single-cation borohydrides. In the alkali-metal mixed compound $\mathrm{LiK(BH_4)_2}$, only a minor change of the dynamical charge is present, and $Z^*_{\rm Li} = +1.01$ on lithium is closer to its nominal value than on the potassium cation (+1.1).

In the compounds containing alkali metal and metals such as Sc or Al, the Born effective charge on the alkali metal shows larger variation than for the LiK compound, i.e., +1.22 for Na, +1.28 for K, in the system with Sc; $Z^*_{\rm K} = +1.26$ for $\mathrm{KAl(BH_4)_4}$. The Born effective charge on the second cation in these compounds is strongly modified: for Sc it is reduced below the nominal value to +2.43 in $\mathrm{NaSc(BH_4)_4}$ and +2.65 in $\mathrm{KSc(BH_4)_4}$, and enhanced to +2.16 for $\mathrm{KAl(BH_4)_4}$. In the above cases, the charge is closer to the nominal value than for respective single-cation borohydrides.

In the mixed-cation mixed-anion borohydride $\mathrm{NaY(BH_4)_2Cl_2}$, the dynamical charges are respectively larger ($Z^*_{\rm Na} = +1.29$) and smaller ($Z^*_{\rm Y} = +3.16$) than the respective values in the single-phase compounds. Also for this compound the Z^* of yttrium is closer to the nominal value than in the $\mathrm{Y(BH_4)_3}$; however, it is still larger than +3.

The static charges for all compounds studied here are smaller than the nominal values. The difference is smallest for the alkali metals and it increases with the increasing valency of the metal cations. The static Bader charges differ from the Born effective charges. For the compounds with Ca, and especially for Sc and Y cations, the dissimilarity between Bader and Born charges is pronounced; moreover, they are smaller or larger than formal charges. The origin of this discrepancy will be discussed in the following paragraph. One shall note that contrary to the static charge, the dynamical one contains contribution from the electronic polarization effects induced by an atomic displacement and related to the site symmetry of a given ion [27]. The symmetry of the atomic orbitals is associated to the site symmetry of the ion in the crystalline structure, therefore, we proceed to the analysis of the electronic structure.

The partial electronic densities of states (PDOS) for three selected metal borohydrides with Born effective charges that are close to nominal (KBH_4), larger than nominal [$\mathrm{Y(BH_4)_3}$],

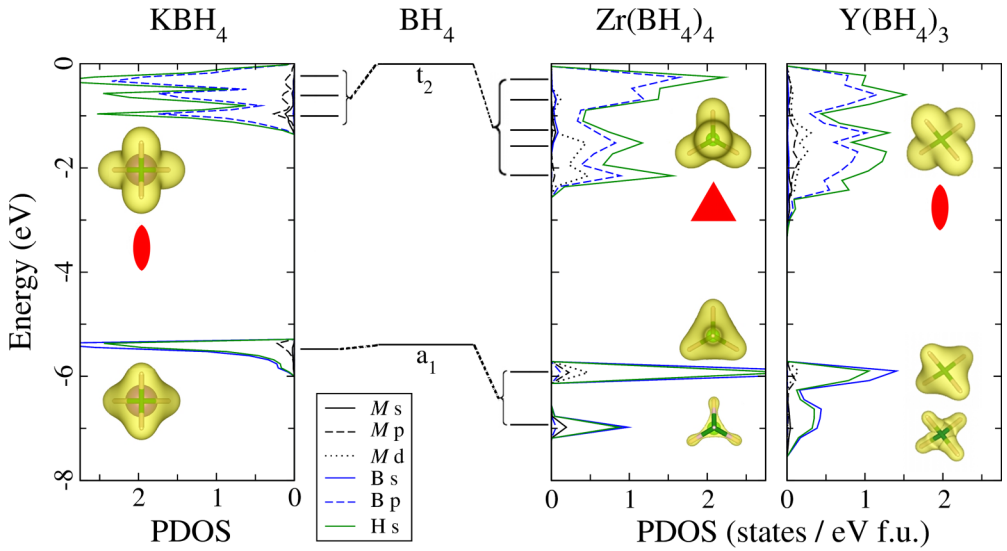

FIG. 2. (Color online) Schematic molecular orbital diagram for BH_4, and partial densities of states PDOS for K-, Y-, and Zr-borohydrides. The origin of the energies corresponds to the top of valence states. Insets show the density of electronic states on BH_4 related to the energy range of the bottom and top of the valence band. Electron density is plotted for isosurfaces at 0.03 and 0.0125 e/Å^3, respectively. Red symbols are used to indicate the twofold and threefold symmetry axes.

and smaller than nominal $[Zr(BH_4)_4]$ are presented in Fig. 2. The molecular orbital (MO) diagram for undistorted $[BH_4]^-$ is analogous to that for methane CH_4. It consists of two orbitals: the lower one in the energy scale corresponds to the a_1 (ss) symmetry that is a combination of H-1s and B-2s orbitals; the higher one in the energy scale triply degenerated t_2 (sp^3) state results from the combination of B-2p and H-1s orbitals (see Fig. 2). For BH_4 embedded in a crystalline metal borohydride, the sp^3 degeneracy can be removed once the site symmetry of the boron atom does not follow the symmetry of the orbital. This is observed for PDOS of the three compounds in Fig. 2; however, only for strongly ionic KBH_4 the triple degeneracy of the sp^3 orbital is removed, while deeper a_1 states are not affected, as presented in the left part of Fig. 2. The inset shows the electronic density related to a_1 and t_2 orbitals as seen from the cation position. BH_4 is in a bidentate orientation with respect to the cation. No distortion of electron density is observed for both orbitals.

In $Y(BH_4)_3$ the anions are also in the bidentate orientation with respect to the Y cation. The tetrahedral geometry T_d of the BH_4 anion is lowered to the C_{2v} symmetry; the difference between the shortest and longest B-H bonds Δd does not exceed 0.5%. Because of the interactions with Y orbitals, two distinctive peaks appear in the lower part of the energy related to a_1 states, which are centered at about -6.7 and -5.9 eV. Figure 2 shows also that the electronic cloud of both s-p hybridization and those of deeper states are symmetrically distributed in the BH_4 units. Owing to the site symmetry in $Y(BH_4)_3$, changes in the polarization of the BH_4 orbitals resulting from the relative cation-anion displacement can propagate along the M-B bonds, leaving the effective charge on the metal above the nominal value.

$Zr(BH_4)_4$ is composed of molecular units with a dominant covalent character of the bonds. The crystalline structure is formed because of van der Waals interactions. The central cation has a T_d symmetry, while the anions surrounding it are distorted (compressed by about 4.5%) along their c_3 axes. Because of the interaction with zirconium d and s orbitals, the bands derived from the BH_4 a_1 orbitals split into two peaks centered at about -6.9 ($1a_1$) and -5.9 eV ($1t_2$). As can be seen in Fig. 2, the electron densities related to these states are strongly polarized towards the central cation. For the symmetry reason, the displacement of the Zr atom towards one of the BH_4 anions (apical one) leads to a different charge rearrangement on this anion than the electronic polarization on the remaining three BH_4 in the basal plane. Here, the depletion of the effective charge is related both to the site symmetry of the central cation and the discrete structure of the compound.

Since the effective charges presented in Fig. 1 are affected by the local symmetry of the cations, it is instructive to look at the coordination of the cation by the BH_4 units. Although for alkali-metal borohydrides the coordination number (CN) is either 4 (Li) or 6 (Na, K), these compounds exhibit the predominantly ionic character of the M-BH_4 interaction [7], therefore Z^* does not depart substantially from the nominal charge. For $Ca(BH_4)_2$, Sc- and $Y(BH_4)_3$, where the cationic effective charges are larger than the nominal ones, the CN is 6. For the compounds with lower CN, $Mg(BH_4)_2$ (CN = 4), $Zr(BH_4)_4$ (CN = 4), $Al(BH_4)_3$ (CN = 3), and $Be(BH_4)_2$ (CN = 3), the effective charges are lower than the nominal ones. Similarly to $Zr(BH_4)_4$, the crystal structures of $Be(BH_4)_2$ and $Al(BH_4)_3$ are composed of $M(BH_4)_n$ molecular units that are, however, arranged in chains. This type of the crystal structure indicates a weak bonding between chains and a stronger bonding within the molecular units. Indeed, the electronic structure and charge-density analysis through the first-principles calculations by Van Setten and de Wijs have shown [50] that the Be atoms in $Be(BH_4)_2$ are involved in the covalent bonding within the polymer backbone.

In the bialkali borohydride $LiK(BH_4)_2$, the Li cation retains the tetrahedral coordination by BH_4 groups, but CN

of K increases to seven. Accordingly, the effective charge on K increases when compared to that in the single-cation compound. The cations in $NaY(BH_4)_2Cl_2$ preserve their sixfold coordination by 4 BH_4 and 2 Cl (Na), and by 2 BH_4 and 4 Cl (Y), respectively. However, here the substitution of the tetrahydroborate anions by chloride might affect the values of dynamical charges. The increased CN of both Al from 3 in $Al(BH_4)_3$ to 4 in $KAl(BH_4)_4$, and K from 6 in KBH_4 to 8 in the mixed compound leads to enhanced Z^*_M. For both $KSc(BH_4)_4$ and $NaSc(BH_4)_4$, the CN of a heavier atom is lower when compared to that in $Sc(BH_4)_3$ (CN = 4 and 6, respectively), and accordingly the value of Z^*_{Sc} is lower than the nominal charge of +3. The effective charges on alkali metals are similar among compounds containing the complex anions, i.e., $[Al(BH_4)_4]^-$ and $[Sc(BH_4)_4]^-$.

B. Ionic potential

Following Fajans' concept of the formation of polar-covalent → covalent bonds via the progressive polarization of the idealized ionic ones [19], a covalent bond can be viewed as an extreme polarization of the charge between the ions to such an extent that the electrons are getting shared between them. Large charges and small sizes of the cations increase the bond polarization [19]. The charge-to-size ratio (the ionic potential [18]) measures the magnitude of the electron cloud distortion of an anion.

As early as in the 1950s, it was shown that the stabilities of diverse compounds sharing a common anion, i.e., oxides, halogens, sulfides, and nitrides, are related to the ionic potential of cations [21]. The inverse relationship between thermal stability and the ionic potential in zeolites has been revealed recently by Cruciani [22]. While in the aforementioned studies the nominal charge of the cations has been utilized to derive the ionic potential, in this study we employ both the static Bader and dynamical Born effective charges to calculate the ionic potentials of cations. Let us recall that Z^* indicates a different degree of the ionic/covalent character of bonds. The values of dynamical charges are related to the electronic charge rearrangement induced by an atomic displacement. Only within an extreme ionic limit, and for a rigid-ion picture, the dynamical charge coincides with the nominal static one of the ion. When the material is partially covalent, the displacement of a given ion induces a nonrigid displacement of the associated electronic charge, leaving non-nominal values of the dynamical charges. Whether they fall above or below the nominal charge depends on the local symmetry of the ions, as discussed in the preceding section. The coordination number for metal atoms increases with their ionic radii. Small Be and Al ions exhibit trigonal-planar coordination by BH_4 units (CN = 3). Tetrahedral coordination is observed for Li, Mg, and Zr. For the largest cations Sc, Y, Ca, Na, and K, the coordination number increases to 6 (octahedral coordination). In $LiK(BH_4)_2$, the potassium cation is even seven-coordinated (coordination environment is a capped trigonal prism). The Shannon crystal and ionic radii [24] (see Table S8 of the Supplemental Material [47]) along with the calculated effective charges of metal cations have been used to calculate the ionic potentials.

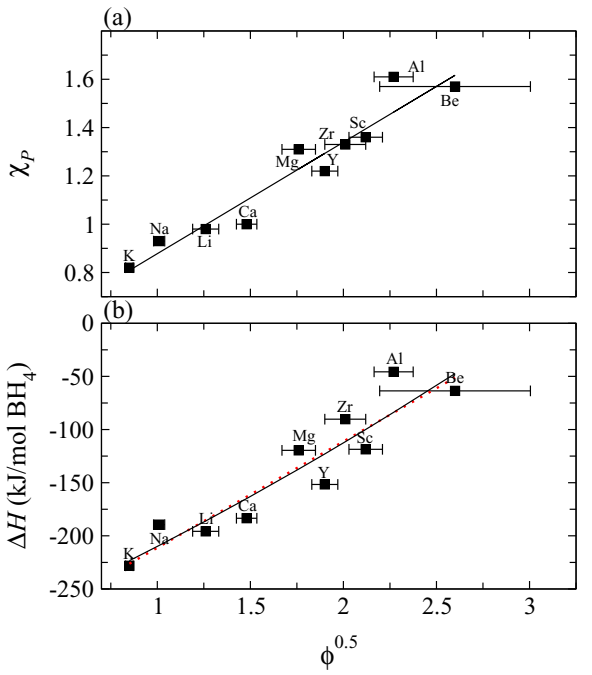

FIG. 3. (Color online) The correlation between Pauling electronegativity χ_P and the square root of the metal ionic potential $\phi^{0.5}$ for the single-cation borohydrides obtained using dynamical charges (a). The heat of formation ΔH of $M(BH_4)_n$ as a function of $\phi^{0.5}$ (b). The uncertainty of the calculated ionic potential results from using both the Shannon crystal and ionic radii. The ionic potentials calculated employing the Shannon crystal radii are lower than those obtained using the ionic radii. The linear and quadratic fits are shown by the dotted (red) and solid (black) lines, respectively, once they are distinguishable.

In Fig. 3, we present the square root of the metal ionic potential versus Pauling electronegativity for single-cation borohydrides. There is a strong linear correlation between $\phi^{0.5}$ and χ_P, the Pearson correlation coefficient is 0.94. Using first principles, Nakamori *et al.* [7] have calculated the heats of formation for a set of single-cation borohydrides and plotted them against the Pauling electronegativity of cations. They have shown that ΔH of $M(BH_4)_n$ scales linearly with the χ_P of a metal. The linear ΔH dependence on χ_P might seem surprising taking into account that Pauling in his thermochemical approach to electronegativity [15,16] pointed out that the energy of heteroatomic bonds $D(A\text{-}B)$ is related to the difference between the electron-attracting abilities of A and B by the relation $\chi_A - \chi_B \propto \{D(A\text{-}B)\text{–}[D(A\text{-}A) + D(B\text{-}B)]/2\}^{0.5}$. For salt MX_n, where X is an anion, $\chi_A - \chi_B \propto (-\Delta H/n)^{0.5}$ [16,17]. Since the difference in the atoms' electronegativity can be regarded as a measure of the degree of electron transfer between the atoms on the chemical bond formation, the ionic potential can serve as an electronegativity measure. Figure 3 also shows the calculated heats of formation of $M(BH_4)_n$ plotted against the square root of the metal ionic potential. Our results for ΔH are in a very good agreement with Nakamori *et al.* [7]. Both the linear $y = -311.29 + 100.05x$ and quadratic $y = -293.35 + 76.32x + 7.04x^2$ (where $y \equiv \Delta H$ and $x \equiv \phi^{0.5}$) fit describe the ΔH on $\phi^{0.5}$ dependence equally well. As one can see in Fig. 3, both regression

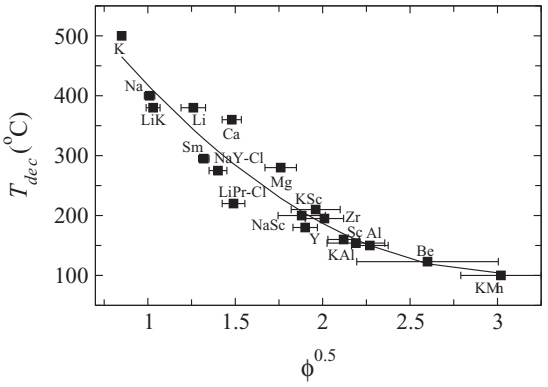

FIG. 4. The experimental decomposition temperatures T_{dec} as a function of $\phi^{0.5}$ obtained using dynamical charges on cations (cf. Fig. 3). The regression line has been fitted using second-degree polynomial.

lines coincide for the range of ionic potential considered here.

The experimental decomposition temperature as a function of the square root of the metal ionic potential for series of $M(\mathrm{BH_4})_n$ and $MM'(\mathrm{BH_4})_n$ is presented in Fig. 4. In Fig. S3 of the Supplemental Material [47], we show both the linear and quadratic regression lines for the T_{dec} dependence on $\phi^{0.5}$. The second-degree polynomial ($y' = 795.36 - 451.46x + 73.64x^2$, $y' \equiv T_{\mathrm{dec}}$) describes the correlation between the experimental T_{dec} and $\phi^{0.5}$ better than the linear regression ($y' = 566.29 - 178.49x$). The decomposition temperature of $\mathrm{LiBH_4}$ is from Ref. [51]; T_{dec} of the remaining alkali-metal borohydrides and also Mg-, Sc-, and Zr- borohydrides are from Ref. [10]; for $\mathrm{Ca(BH_4)_2}$ we adopt data from Ref. [40]; T_{dec} for $\mathrm{KAl(BH_4)_4}$ is from Ref. [12]; those for $\mathrm{Sm(BH_4)_2}$ and $\mathrm{LiPr(BH_4)_3Cl}$ are from Ref. [13]; T_d for $\mathrm{K_2Mn(BH_4)_4}$ is from Ref. [52]; the remaining data are from Ref. [2] and the references therein.

The strongly ionic alkali-metal borohydrides are the most stable against the decomposition. The charges on cations in this group of tetrahydroborates are very close to the formal charge of +1. However, Li has the smallest ionic radius among the group-I alkali metals (0.59 Å in the fourfold-coordinated versus 1.02 and 1.38 Å, respectively, for Na and K in the sixfold-coordinated polyhedra in $M\mathrm{BH_4}$), which implies its larger polarizing ability when compared to Na and K. Stronger polarizing power of the Li, in comparison to K, cation in the $M\mathrm{BH_4}$ compounds is also recognizable in the the electron localization function (ELF) contour plots shown in Fig. S2 of the Supplemental Material [47]. The decreasing stability of metal borohydrides follows the increasing polarizing ability of the cation. $\mathrm{Be(BH_4)_2}$ is one of the least stable among the compounds studied here due to the high charge-to-size ratio of the Be ion that strongly polarizes the bonds.

In Fig. S3 of the Supplemental Material [47], we also plot the square root of ionic potentials obtained employing static charges of cations versus the experimental decomposition temperatures. Let us recall that while the static charges of cations in all compounds considered here are lower than the metal formal charge, the dynamical ones are close to, smaller, or larger than the formal charge, depending on the bonding properties and the site symmetry of a given material. The dynamical charges on the octahedrally coordinated cations in Y- and $\mathrm{Sc(BH_4)_3}$ are larger than both their nominal value of +3 and the values of static charges. For these compounds, the quadratic correlation between the stability-square root of ionic potential breaks if the Bader charges are used.

The stabilities of the bimetallic borohydrides $\mathrm{LiK(BH_4)_2}$, $\mathrm{NaY(BH_4)_2Cl_2}$, and $\mathrm{LiPr(BH_4)_3Cl}$ are determined by a geometrical mean of the ionic potentials of both cations. For the bialkali borohydride, we take into account the increased potassium ionic radius in seven-coordinated polyhedra. In contrast, in the mixed-metal borohydrides containing complex anions T_{dec} depends on the $\phi^{0.5}$ of the complex-anion-forming metal. This demonstrates that the covalently bonded complex anions play a key role in the structural stability of this group of compounds [2].

IV. CONCLUDING REMARKS

Using a state-of-the-art DFT method we provide insight into the physical mechanism determining the stabilities of a technologically significant class of tetrahydroborates. The stabilities of metal borohydrides have been found to follow the quadratic correlation between the experimental decomposition temperatures and the square root of ionic potential of the cations.

The ionic potential has been calculated as the cation's charge-to-size ratio in coordinated anion polyhedra around the cation. The charge on the cation in metal borohydrides shows a departure from its formal value if the ionic character of the M-$\mathrm{BH_4}$ interaction decreases. While the static Bader charges fall below the formal ones, the values of dynamical charges can be close to, smaller, or larger than the formal metal valence, depending on the bonding properties and the site symmetry of a given compound. Accordingly, the quadratic relationship between thermal stabilities of the metal borohydrides and $\phi^{0.5}$ of the metal cations holds if the ionic potential is calculated using dynamical charges.

To summarize, the departure of the effective charge on a metal atom from its formal valence in borohydrides shows that the strength of the coordinative bonding between metal cation and the tetrahydroborate anions is the dominant factor in determining their stabilities. This is also the case of mixed-metal borohydrides containing complex anions, in which the covalently bonded complex anions play a key role in the structural stability of the compounds.

ACKNOWLEDGMENT

Financial support by a grant from Switzerland through the Swiss Contribution to the enlarged European Union and CPU allocation at the PL-Grid Infrastructure are gratefully acknowledged.

[1] H.-W. Li, Y. Yan, S.-i. Orimo, A. Züttel, and C. M. Jensen, Energies **4**, 185 (2011).

[2] L. H. Rude, T. K. Nielsen, D. B. Ravnsbæk, U. Bösenberg, M. B. Ley, B. Richter, L. M. Arnbjerg, M. Dornheim, Y. Filinchuk, F. Besenbacher, and T. R. Jensen, Phys. Status Solidi A **208**, 1754 (2011).

[3] K. Miwa, N. Ohba, S.-i. Towata, Y. Nakamori, and S.-i. Orimo, Phys. Rev. B **69**, 245120 (2004).

[4] P. Vajeeston, P. Ravindran, A. Kjekshus, and H. Fjellvåg, J. Alloys Compd. **387**, 97 (2005).

[5] E. Orgaz, A. Membrillo, R. Castañeda, and A. Aburto, J. Alloys Compd. **404–406**, 176 (2005).

[6] K. Miwa, M. Aoki, T. Noritake, N. Ohba, Y. Nakamori, S.-i. Towata, Andreas Züttel, and S.-i. Orimo, Phys. Rev. B **74**, 155122 (2006).

[7] Y. Nakamori, K. Miwa, A. Ninomiya, H. Li, N. Ohba, S.-i. Towata, A. Züttel, and S.-i. Orimo, Phys. Rev. B **74**, 045126 (2006).

[8] H.-W. Li, S.-i. Orimo, Y. Nakamori, K. Miwa, N. Ohba, S. Towata, and A. Züttel, J. Alloys Compd. **446–447**, 315 (2007).

[9] Z. Łodziana, P. Błoński, Y. Yan, D. Rentsch, and A. Remhof, J. Phys. Chem. C **118**, 6594 (2014).

[10] E. A. Nickels, M. O. Jones, W. I. David, S. R. Johnson, R. L. Lowton, M. Sommariva, and P. P. Edwards, Angew. Chem. Int. Ed. **47**, 2817 (2008).

[11] D. R. Ravnsbæk, M. B. Ley, Y. S. Lee, H. Hagemann, V. D'Anna, Y. W. Cho, Y. Filinchuk, and T. R. Jensen, Int. J. Hydrogen Energy **37**, 8428 (2012).

[12] D. A. Knight, R. Zidan, R. Lascola, R. Mohtadi, Ch. Ling, P. Sivasubramanian, J. A. Kaduk, S.-J. Hwang, D. Samanta, and P. Jena, J. Phys. Chem. C **117**, 19905 (2013).

[13] J. E. Olsen, Ch. Frommen, T. R. Jensen, M. D. Riktor, M. H. Sørbya, and B. C. Hauback, RSC Adv. **4**, 1570 (2014).

[14] S. Carniato, L. Journel, R. Guillemin, M. N. Piancastelli, W. C. Stolte, D. W. Lindle, and M. Simon, J. Chem. Phys. **137**, 144303 (2012).

[15] L. Pauling, J. Am. Chem. Soc. **54**, 3570 (1932).

[16] L. Pauling, *The Nature of The Chemical Bond*, 3rd ed. (Cornell University Press, Ithaca, NY, 1960).

[17] A. L. Allred, J. Inorg. Nucl. Chem. **17**, 215 (1961).

[18] G. H. Cartledge, J. Am. Chem. Soc. **50**, 2855 (1928).

[19] Summarized in K. Fajans, *Radioelements and Isotopes, Chemical Forces and the Optical Properties of Substances* (McGraw-Hill, New York, 1931).

[20] W. B. Jensen, J. Chem. Educ. **89**, 94 (2011).

[21] G. H. Cartledge, J. Phys. Chem. **55**, 248 (1951).

[22] G. Cruciani, J. Phys. Chem. Solids **67**, 1973 (2006).

[23] L. Pauling, J. Am. Chem. Soc. **51**, 1010 (1929).

[24] R. D. Shannon, Acta Crystallogr. **A32**, 751 (1976).

[25] R. Bader, *Atoms in Molecules: A Quantum Theory* (Oxford University Press, New York, 1990).

[26] M. Born and M. Goeppert-Mayer, Handb. Phys. **24**, 623 (1931); M. Born and K. Huang, *Dynamical Theory of Crystal Lattices* (Oxford University Press, Oxford, UK, 1954).

[27] Ph. Ghosez, J.-P. Michenaud, and X. Gonze, Phys. Rev. B **58**, 6224 (1998).

[28] R. Resta, Rev. Mod. Phys. **66**, 899 (1994).

[29] W. Kohn and L. Sham, Phys. Rev. **140**, A1133 (1965).

[30] G. Kresse and J. Furthmüller, Comput. Mater. Sci. **6**, 15 (1996); Phys. Rev. B **54**, 11169 (1996).

[31] G. Kresse and D. Joubert, Phys. Rev. B **59**, 1758 (1999).

[32] P. E. Blöchl, Phys. Rev. B **50**, 17953 (1994).

[33] J. P. Perdew, K. Burke, and M. Ernzerhof, Phys. Rev. Lett. **77**, 3865 (1996).

[34] H. J. Monkhorst and J. D. Pack, Phys. Rev. B **13**, 5188 (1976).

[35] J.-P. Soulié, G. Renaudin, R. Černý, and K. Yvon, J. Alloys Compd. **346**, 200 (2002).

[36] O. A. Babanova, A. V. Soloninin, A. P. Stepanov, A. V. Skripov, and Y. Filinchuk, J. Phys. Chem. C **114**, 3712 (2010).

[37] G. Renaudin, S. Gomes, H. Hagemann, L. Keller, and K. Yvon, J. Alloys Compd. **375**, 98 (2004).

[38] D. S. Marynick and W. N. Lipscomb, Inorg. Chem. **11**, 820 (1972).

[39] J. Voss, J. S. Hummelshøj, Z. Łodziana, and T. Vegge, J. Phys.: Condens. Matter **21**, 012203 (2009).

[40] Y. Filinchuk, E. Rönnebro, and D. Chandra, Acta Mater. **57**, 732 (2009).

[41] S. Aldridge, A. J. Blake, A. J. Downs, R. O. Gould, S. Parsons, and C. R. Pulham, J. Chem. Soc., Dalton Trans.1007 (1997).

[42] Z. Łodziana, Phys. Rev. B **81**, 144108 (2010).

[43] T. Sato, K. Miwa, Y. Nakamori, K. Ohoyama, H.-W. Li, T. Noritake, M. Aoki, S.-i. Towata, and S.-i. Orimo, Phys. Rev. B **77**, 104114 (2008).

[44] L. H. Rude, M. Corno, P. Ugliengo, M. Baricco, Y.-S. Lee, Y. W. Cho, F. Besenbacher, J. Overgaard, and Torben R. Jensen, J. Phys. Chem. C **116**, 20239 (2012).

[45] R. Černý, G. Severa, D. B. Ravnsbæk, Y. Filinchuk, V. D'Anna, H. Hagemann, D. Haase, C. M. Jensen, and T. R. Jensen, J. Phys. Chem. C **114**, 1357 (2010).

[46] R. Černý, D. B. Ravnsbæk, G. Severa, Y. Filinchuk, V. D'Anna, H. Hagemann, D. Haase, J. Skibsted, C. M. Jensen, and T. R. Jensen, J. Phys. Chem. C **114**, 19540 (2010).

[47] See Supplemental Material at http://link.aps.org/supplemental/10.1103/PhysRevB.90.054114 for the convergence of the Born effective charge tensor (BECT) calculations; components of BECT; the electron localization contour plots for selected metal borohydrides; the values of ionic and crystal radii employed in the calculations of the ionic potentials; and the Pauling electronegativity and the experimental decomposition temperatures as a function of the square root of the cation ionic potential.

[48] G. Henkelman, A. Arnaldsson, and H. Jónsson, Comput. Mater. Sci. **36**, 254 (2006).

[49] E. Sanville, S. D. Kenny, R. Smith, and G. Henkelman, J. Comput. Chem. **28**, 899 (2007).

[50] M. J. van Setten, G. A. de Wijs, and G. Brocks, Phys. Rev. B **77**, 165115 (2008).

[51] P. Mauron, F. Buchter, O. Friedrichs, A. Remhof, M. Bielmann, Ch. N. Zwicky, and A. Züttel, J. Phys. Chem. B **112**, 906 (2008).

[52] R. Liu and D. Book, Int. J. Hydrogen Energy **39**, 2194 (2014).